Cell, Vol. 41, 933–943, July 1985, Copyright © 1985 by MIT 0092–8674/85/070933–11 $02.00/0

DNA Gyrase and Its Complexes with DNA: Direct Observation by Electron Microscopy

T. Kirchhausen, J. C. Wang, and S. C. Harrison
Department of Biochemistry and Molecular Biology
Harvard University
7 Divinity Avenue
Cambridge, Massachusetts 02138

Summary

Electron microscopy of DNA gyrase holoenzyme, of gyrase A subunits, and of the complexes of both species with DNA enables us to deduce the relative locations of subunits in the holoenzyme and to indicate a plausible path for DNA complexed with gyrase. The structural results are discussed in terms of certain models for directional DNA strand transport.

Introduction

DNA gyrase was first identified by Gellert et al. (1976) as a factor of E. coli extracts needed to support in vitro integrative recombination of phage λ DNA. It is required when the DNA substrate is in a relaxed circular form (Nash et al., 1977). Gyrase catalyzes negative supercoiling of DNA coupled to ATP hydrolysis (Gellert et al., 1976) by allowing a double-stranded DNA segment to pass through an enzyme-bridged, transient double-stranded break (Cozzarelli, 1980; Gellert, 1981a). That is, gyrase generates a 'gate' and actively transports one DNA segment across another. The transport is directional or vectorial when coupled to ATP hydrolysis, so that the linking number of the duplex DNA ring is always reduced. Bacterial gyrase, phage T4 DNA topoisomerase, and eukaryotic DNA topoisomerase II all catalyze the breakage and resealing of a pair of DNA strands in concert to permit the passage of one DNA segment through another; these enzymes are classified as type II DNA topoisomerases (Liu et al., 1980; Cozzarelli, 1980; Gellert, 1981a, 1981b; Wang, 1982, 1985). Bacterial gyrase is, however, the only known type II topoisomerase that can catalyze directional strand transport. Gyrase thus carries out an elaborate sequence of operations in a way that governs long-range topological properties of DNA.

The experiments showing that the supercoiling reaction of gyrase involves DNA strand passage through an enzyme-bridged transient break are important in considering models for its mechanism. Treatment of DNA–DNA gyrase complex with protein denaturants shows directly that there is a double-strand break in the DNA (Sugino et al., 1977; Gellert et al., 1977). The break is staggered by four bases (Morrison and Cozzarelli, 1979, 1981; Kirkegaard and Wang, 1981; Fisher et al., 1981), with an A subunit attached by a tyrosyl-phosphate linkage to each of the 5′-protruding DNA ends (Tse et al., 1980; Sugino et al., 1980). Strand passage through this break is implicit in the observation that gyrase changes the DNA linking number in steps of two, both in the supercoiling reaction and in an ATP-independent relaxation reaction (Brown and Cozzarelli, 1979; Mizuuchi et al., 1980). The knotting/unknotting and catenation/decatenation of covalently closed double-stranded DNA rings by the enzyme also require a transient double-strand break (Kreuzer and Cozzarelli, 1980; Mizuuchi et al., 1980).

DNA gyrase is composed of two subunits, designated A and B, the products of the *gyr* A and *gyr* B genes, respectively. For either the E. coli or M. luteus enzyme, the molecular mass of each subunit is close to 100,000 daltons, with the A subunit slightly larger than B (see reviews previously cited). The active enzyme is an A_2B_2 tetramer (Klevan and Wang, 1980). Nuclease protection studies of the gyrase–DNA complex reveal an extended region of contact between the enzyme and the DNA. About 140 bp of DNA interact with the protein in a way that protects them from digestion by staphylococcal nuclease. Digestion of the complex with pancreatic DNAase I produces a series of DNA strands differing in size by integral multiples of 10 nucleotides (Liu and Wang, 1978a). These results are reminiscent of nuclease digestion patterns of nucleosomes and support the earlier postulate that in the DNA–DNA gyrase complex, a DNA segment might be wrapped on the surface of the enzyme (Liu and Wang, 1978b). More detailed DNAase I 'footprinting' of strong gyrase binding sites (Kirkegaard and Wang, 1981; Morrison and Cozzarelli, 1981; Fisher et al., 1981) shows that the total length of protected DNA is indeed about 140 bp; the central ~40 bp are quite resistant to DNAase I, and the site of gyrase-mediated double-strand cleavage lies near the center of this region. The flanking sequences on either side of the 140 bp segment show enhanced cleavage at 10–11 bp intervals, with a 2–4 bp stagger for sites on complementary strands (Kirkegaard and Wang, 1981). These flanking 40–50 bp therefore appear to be accessible to DNAase I from only one side of the DNA double helix.

Various models have been proposed to account for the observations summarized above (Brown and Cozzarelli, 1979; Wang et al., 1980; Mizuuchi et al., 1980; Cozzarelli et al., 1980; Kirkegaard and Wang, 1981; Morrison and Cozzarelli, 1981), but lack of a structural picture of gyrase and of its complex with DNA has prevented a more concrete understanding of how the enzyme works. We report here results obtained by electron microscopic examination of gyrase holoenzyme, of the dimer of gyrase A subunit, and of their complexes with DNA. We show that the unique shapes of the A_2B_2 holoenzyme and of the A_2 dimer make it possible to deduce the relative locations of the subunits in the holoenzyme and to indicate a plausible path of DNA segment in the gyrase–DNA complex. The directional DNA strand transport by the enzyme is discussed in light of the present structural information.

Results

Electron Microscopy of Gyrase

Figure 1a shows images of gyrase (from M. luteus) sprayed onto mica and visualized by rotary shadowing

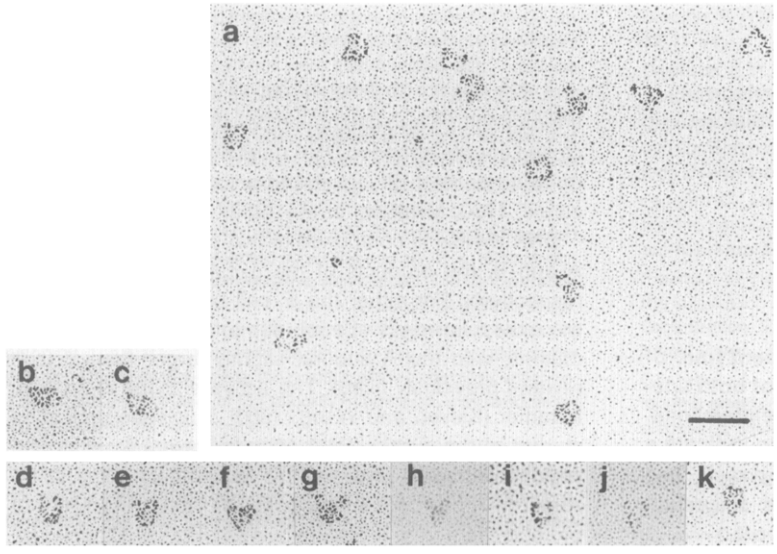

Figure 1. Electron Micrographs of DNA Gyrase from M. luteus Shadowed with Platinum

Outline of molecules is enhanced by rotary shadowing: (a) general field, (b–k) gallery of selected images of shadowed gyrase. These are lozenge (b and c), (bulge) heart (d–g), and (tapered) triangular (h–k) views. Angle of view about the dyad estimated from ear-to-ear separation are: d, 37°; e, 42°; f, 44°; g, 90°; h, 131°; i, 138°; j, 151°; k, 180°. Referring to axes in Figure 2, 180° is a view toward origin along y, and 90° is a view toward origin along x. Bar: 500 Å.

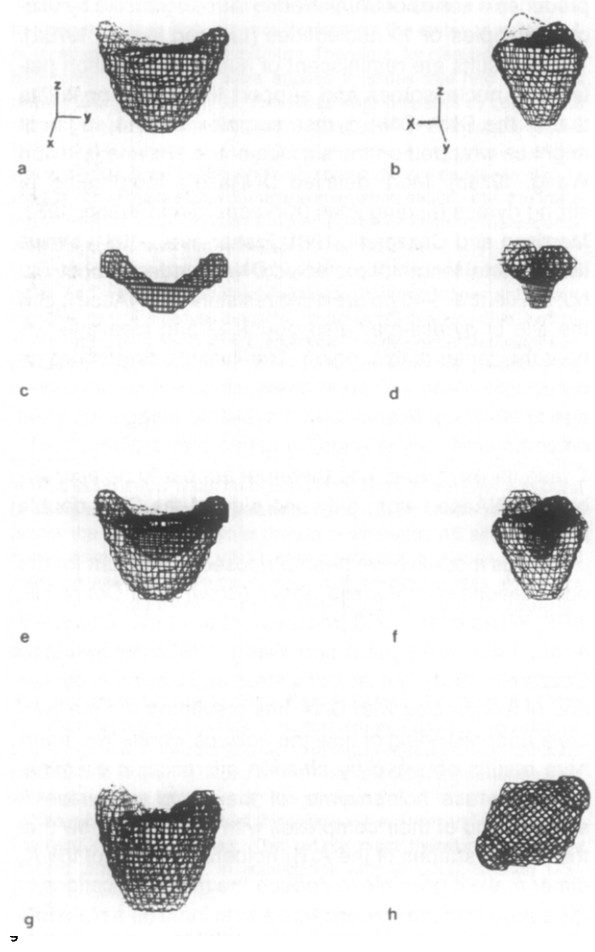

Figure 2. Three-Dimensional Computer Simulation of Gyrase

The model was obtained by a simple direct-space reconstruction of the Pt shadowed outline of the molecule. Its purpose is to facilitate the graphic representation of gyrase. The effective resolution is limited to about 30 Å, and it is affected by Pt grain size and distortions of adsorbed molecule to mica. (a and b) reconstruction of holoenzyme obtained from images of free gyrase. (c and d) reconstruction of A subunit dimer; (e and f) simulation of gyrase, including the reconstruction of the A subunit dimer. (g) Comparison between simulations obtained from images of free gyrase and from gyrase bound to DNA. The small length difference of 20 Å (DNA-gyrase appears taller) is within experimental error. (h) A 'top view' of the model, with a lozenge shape. Note that this gyrase outline was not included in the data set used in the graphic simulation. Axes apply to the orientation of models in a,c,e, and g (view near 90°) and in b,d, and f (view near 180°), respectively. They are the reference frame for angles in Figure 1.

with platinum. We find images that vary in appearance from heart-shaped to lozenge-shaped. Similar micrographs were obtained of gyrase from E. coli (not shown). This apparent shape variability can be accounted for by a gyrase molecule of constant shape that adsorbs with different orientations to the mica surface (see below). Inspection of a large number of pictures shows that a common characteristic of many image outlines is an approximate mirror line that bisects the molecule, suggesting a molecular dyad. Figure 1 is a gallery of images of rotary shadowed gyrase. Figures 1d–1k display molecules with their dyad oriented approximately vertically; these images range in appearance from heart-shaped (Figures 1d–1f) to triangular (Figures 1h–1k). The height from top to bottom is 260–280 Å (this and all other measurements are uncorrected for platinum decoration unless indicated otherwise; since the average diameter of Pt grains in the background of the same fields is 25–30 Å, an estimate for the corrected height is ~210 Å). The presence of a dyad is consistent with previous experiments, which showed that gyrase is a tetramer with an A_2B_2 subunit structure (Klevan and Wang, 1980).

The separation between the 'ears' at the top of the molecule varies with the image and can be up to 270–280 Å (Figure 1g). We show below that much of this variability can be attributed to viewing a molecule of constant shape along different directions. The view angle about the dyad has been estimated from the 'ear-to-ear' separation; it is indicated for each image in the gallery. By using this partial set of views, a three-dimensional model for gyrase has been obtained (Figure 2). The images are equivalent to a

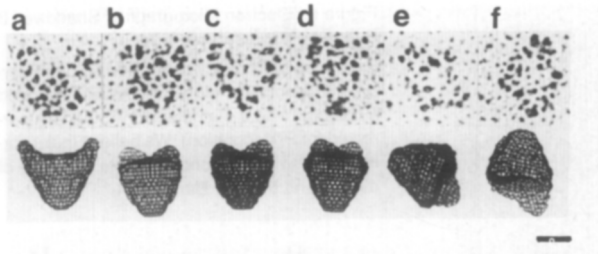

Figure 3. Comparison between Rotary-Shadowed Images of Gyrase and Oblique Views of Simulated Gyrase

Images (a and b) are views normal to the molecular dyad and were included in the data set used in the graphic simulation. The other views were obtained by rigid rotations of the simulation. Bar: 100 Å.

tilt series of projected outlines of the molecule. We have used a simple direct-space reconstruction of the shadowed envelope (see Experimental Procedures) to obtain a convenient three-dimensional representation. Even though the reconstruction is based only on views that we interpret to be normal to the dyad axis, it can nevertheless account for many other images viewed in oblique directions; examples are given in Figure 3. In particular, when the model is projected along its 2-fold axis, it appears as a lozenge with a length of 270–280 Å along its major axis (Figure 2h); this view accounts for the shape of gyrase shown in Figures 1b and 1c.

Electron Microscopy of A Subunit Dimers

The A subunits of DNA gyrase (from M. luteus) yield images with a characteristic 'V' shape when sprayed onto mica and rotary-shadowed with platinum. A field and some selected images are shown in Figure 4. Similar micrographs were obtained of A subunits from E. coli (not shown). Since the A subunits of gyrase are believed to dimerize in solution (Klevan and Wang, 1980), we suggest that each arm of the 'V' corresponds to a single subunit. The maximum separation measured at the top of the 'V' is 270 Å, similar to the maximum separation of the ears at the top of the intact gyrase. The maximum height of the 'V' shape complex is 180 Å, roughly two-thirds the height of the holoenzyme. We have observed a small and limited variation in angular spread of the A subunits (Figures 4b–4f and Figures 4i–4k). We are unsure at present whether this variation corresponds to some flexibility at a hinge between the subunit dimers or to different projected views of the A subunits as they adsorb in various orientations to the mica surface. The latter interpretation is consistent with the presence of some images that appear as single rods with a total length of 270 Å (e.g., Figure 4g). This length is the same as the maximum distance between the ears of intact gyrase (e.g., Figure 1g), and we suggest that this image corresponds to a view of the A dimer along its molecular dyad ('top or bottom view'). Negatively stained images of the A subunits reveal the same 'V' shape assembly seen by rotary shadowing; examples are given in the electron micrographs of Figure 5a. Likewise (Figure 5b), there are putative top views with a characteristic zigzag appearance: two small rods of ~100 Å in length joined at their ends side by side, thus displaying an apparent dislocation (sometimes also seen by rotary shadowing; see Figure 4h).

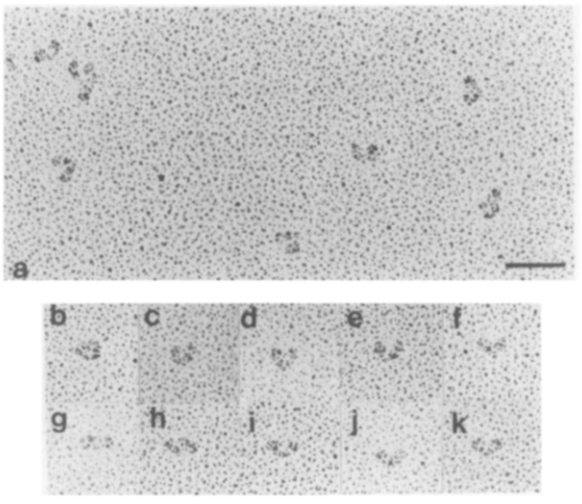

Figure 4. Images of Pt Rotary-Shadowed A Subunit Dimer of Gyrase from M. luteus

(a) Example of a field. (b–k) Selected images: 'V' shaped (b–f, i–k) and extended rods (g and h). Bar: 500 Å.

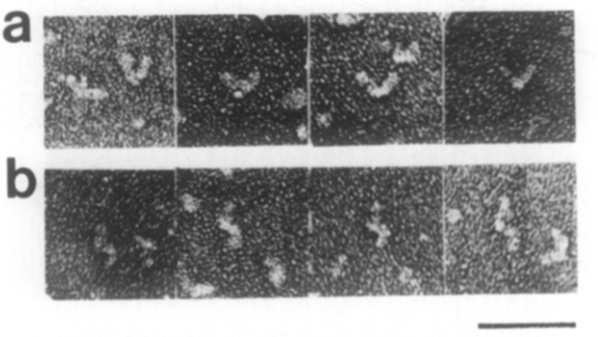

Figure 5. Negatively Stained Images of A Subunit Dimers from M. luteus

(a) Characteristic 'V' shaped assembly; (b) examples of 'zig-zag' appearance, with two offset rods ~100 Å in length (presumptive top view). Bar: 500 Å.

Electron Microscopy of B Subunits

Chemical cross-linking experiments suggest that the B subunit of DNA gyrase purified from M. luteus is monomeric in solution (Klevan and Wang, 1980). The rotary shadowed images of B subunit of E. coli DNA gyrase shown in the electron micrograph of Figure 6 are from a preparation purified from an E. coli strain harboring a multicopy plasmid containing the E. coli *gyr* B gene. Some images show isolated globular structures (indicated by arrow) of about 130 Å in diameter (or about 90 Å if corrected for an estimated Pt grain size of 20 Å). We believe that these correspond to the monomeric species. Other images show what appear to be dimeric, trimeric, and higher-order aggregates of the B subunit.

Complexes with DNA

A general field of a mixture of DNA gyrase and a 541 bp restriction fragment of DNA is shown in Figure 7. Inspec-

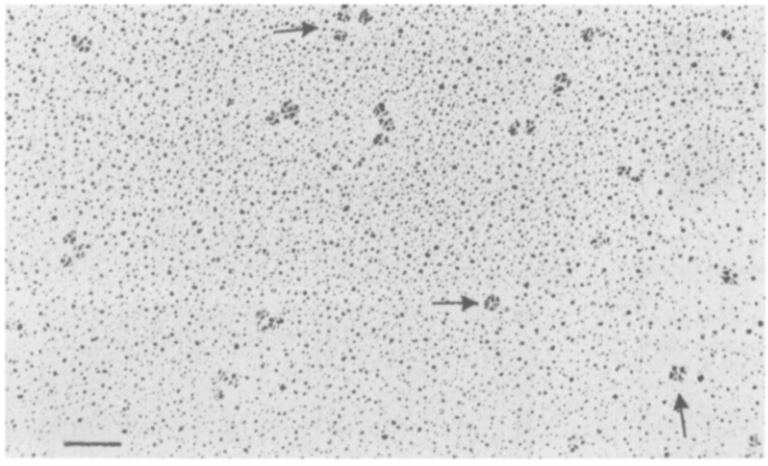

Figure 6. Electron Micrograph of Shadowed B Subunit of Gyrase from E. coli

Examples of Pt rotary-shadowed field of B gyrase. The smallest globular species (indicated by arrows) has a diameter of ~130 Å (not corrected for Pt decoration). We believe that it corresponds to the B monomer. Note presence of dimers and trimers. Bar: 500 Å.

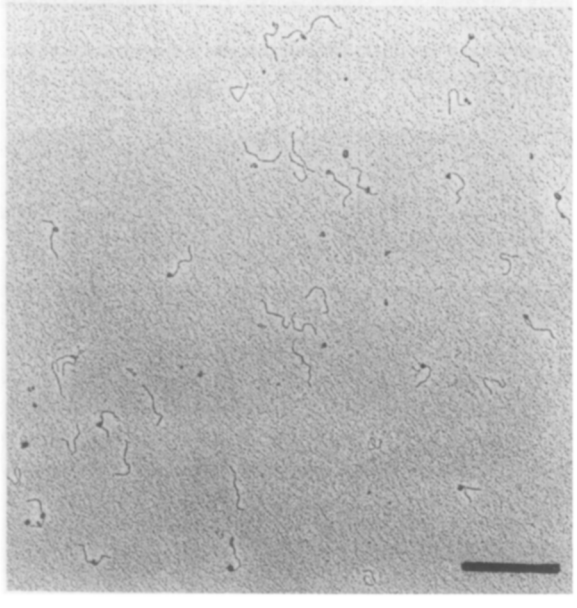

Figure 7. Association of Gyrase from M. luteus with DNA

Field of complexes of gyrase and a 541 bp DNA restriction fragment, glycerol sprayed, adsorbed to mica, and visualized by rotary Pt shadowing. Note that no fixative was used. Bar: 500 Å.

tion of this and other micrographs shows the formation of gyrase–DNA complexes, usually of one DNA fragment with one gyrase molecule. Some free DNA and gyrase can also be found, and the actual yield of complex varies slightly from one experiment to another. Infrequently, we find two DNA fragments associated with the same gyrase. The common characteristic of the 1:1 complexes is that two tails of the bound DNA emerge from the protein. The disposition of the emerging tails varies, however, and we have classified the images into three groups. In the first class both DNA tails emerge from the bottom tip of gyrase; examples of this binding mode are given in Figures 8a, 8b, 8c, 8e, and 8f. We have measured the length of the DNA tails (including the shortest straight distance between their exit points) in a large number of such images and have compared the results with apparent lengths of control DNA. The results, summarized in the histogram of Figure 9b, show that in the majority of the complexes, DNA must be wrapped onto or within the heart-shaped gyrase with a mean apparent shortening of 115 bp. Alternatively, the protected DNA length, calculated from the difference of free DNA and emerging tails in these complexes is 161 ± 6(24) bp. This measurement is in reasonable agreement with the results of nuclease protection and footprinting experiments that have indicated an interaction of 145–155 bp DNA with gyrase (Liu and Wang, 1978a; Kirkegaard and Wang, 1981; Morrison and Cozzarelli, 1981; Fisher et al., 1981). We refer to this class of images as the 'full' binding mode. The same histogram, Figure 9b, also shows that in a smaller subset of complexes, there is no detectable DNA shortening. This indicates absence of DNA wrapping and may correspond to nonspecific interactions that lead to complex formation. The second class of images, such as those in Figures 8h–8k, shows DNA emerging from gyrase at the bottom tip and at an upper ear. As indicated in the histogram of Figure 9c, the measured DNA lengths in most of these complexes exhibit no significant decrease if we include in the length the shortest distance between exit points. Such structures most likely represent incomplete binding modes, since protection experiments show that 'complete' interaction involves 145–155 bp (Liu and Wang, 1978a; Kirkegaard and Wang, 1981; Morrison and Cozzarelli, 1981; Fisher et al., 1981). The third class of images includes views of gyrase along the molecular dyad ('top' views). Sometimes the DNA tails emerge from the opposite ends of the lozenge-shape view of gyrase (Figure 8g), with no significant decrease in DNA length (see histogram in Figure 9d). These images would thus correspond to the 'incomplete' binding mode. In others, DNA tails emerge from the same side (Figure 8d), and they show a 115 bp decrease in the length of the DNA, as indicated in the histogram of Figure 9d. The interpretation of these images is somewhat more ambiguous, and we cannot be certain whether they indeed correspond to 'full' binding modes viewed (somewhat obliquely) from the top. Both full and incomplete binding can also be seen on 541 bp cova-

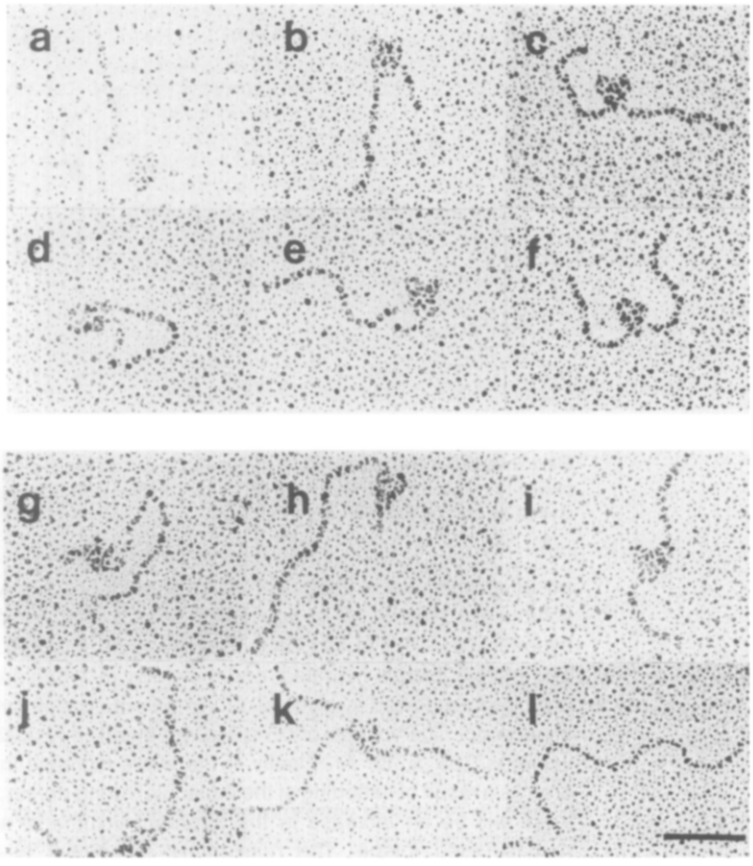

Figure 8. Selected Images of Gyrase Coupled with a 541 bp DNA Restriction Fragment

(a–f) 'Full' binding mode, where DNA tails come from bottom of gyrase; DNA appears shortened by the equivalent of ~115 bp. (g–k) Images with 'half' binding, where DNA tails enter at an upper ear and exit at the bottom tip; no significant decrement in DNA length is found. (d and g) Lozenge-shape view of gyrase complexed to DNA. (l) Free DNA as a control. Bar: 500 Å.

lently closed circles (Figure 10) or with other DNA (a 422 bp fragment and supercoiled and nicked pBR322 plasmid; data not shown).

The gyrase molecule in these complexes is not significantly different in outline from free gyrase. Views normal to the dyad are more frequent, presumably because of the way bound DNA constrains the protein to lie on mica. We have calculated a three-dimensional model using nine images of gyrase bound to DNA in which the enzyme is seen in outline normal to the 2-fold axis. The computer drawing of this representation is shown in Figure 2g, superposed on a similar model for free gyrase. The differences appear to be well within the errors inherent in the measurements and in the computation.

The A subunit dimer binds independently to DNA (Moore et al., 1983; Lother et al., 1984) as shown in Figure 11. In most cases, there is a symmetrical disposition of the DNA tails emerging from the ears across the dyad of the 'V' shaped complex with no significant change in DNA length (Figures 11a–11f and the histogram shown in Figure 12b). This binding is consistent with symmetry requirements of the double-stranded cut made by gyrase, which leaves one A subunit attached to each newly generated 5′ end (Tse et al., 1980; Sugino et al., 1980). Other views, which also do not show DNA shortening, have DNA tails emerging at opposite ends of the 270 Å rods (Figures 11h and 11i); these we think correspond to 'top' views of the dimer. In a few instances, DNA tails emerge from only one end of the complex (Figure 11g), but the number of images is too limited for a meaningful interpretation.

Discussion

The Arrangement of Subunits in DNA Gyrase

The computer graphics representation in Figure 2 summarizes our interpretation of the micrographs of the A_2B_2 gyrase holoenzyme. In making this interpretation, we have assumed that the different images correspond to different views of a single structure and that the outline of this structure is not grossly distorted by drying and shadowing. The absence of major distortion is borne out by the consistency of the images; in particular, although the model is based only on views normal to the dyad, projections of the model along and oblique to the dyad can account for other observed images of the holoenzyme.

The most significant distortion is expected to arise from flattening of the molecules on the mica surface. The molecular volume of the model in Figure 2 is 1.5×10^6 Å^3. The volume expected for 400 kd of 'dry' protein is about 0.5×10^6 Å^3. Several factors probably contribute to the difference. First, the correction for Pt decoration may be too small. Second, there are likely to be significant corrugations and volumes not represented by the envelope as computed (see Experimental Procedures). For example, there must be internal space for 120 to 140 bp of DNA, since the images of gyrase with DNA bound can be super-

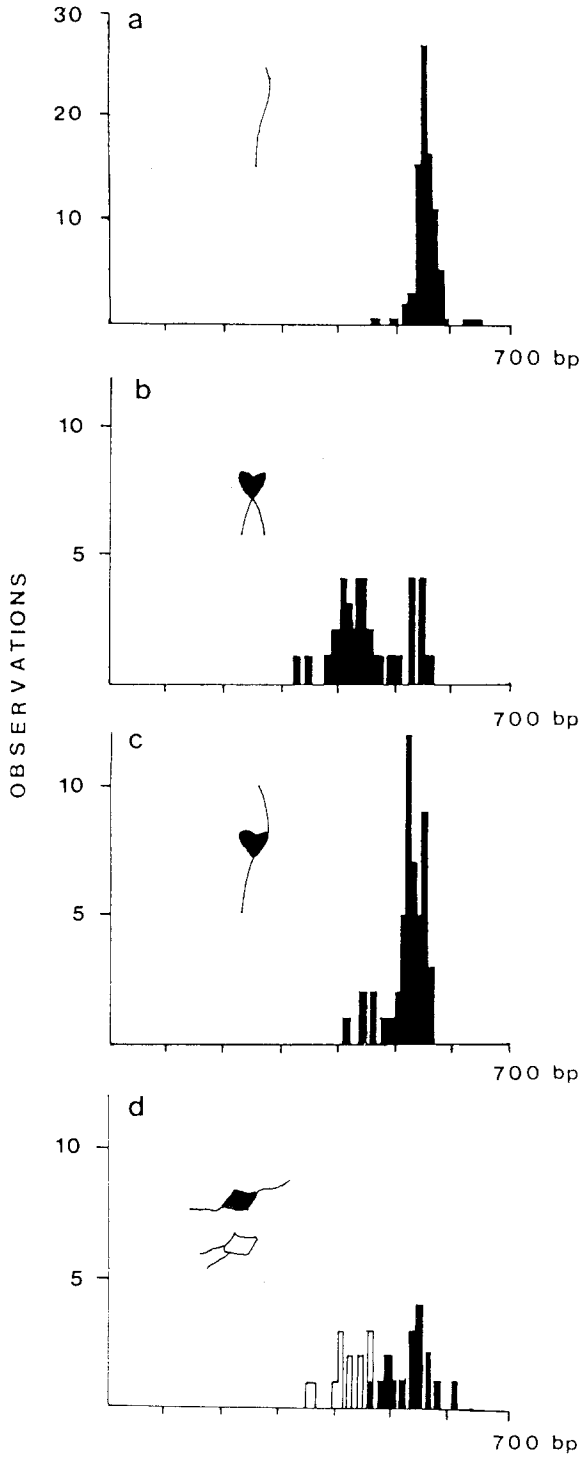

Figure 9. Histograms Showing Distribution of DNA Length When Complexed to Intact Gyrase

Lengths along the 541 bp restriction fragment were measured on tracings; the reported lengths include the shortest straight distance between the points where DNA 'tails' exit from gyrase. Length counts were accumulated in 31.6 Å increments; the ends of DNA molecules were not corrected for Pt decoration. Ordinate indicates number of observations. (a) Length distribution of control DNA used in experiments with gyrase. Average length is 1895 Å (or 3.5 Å/bp). (b) DNA complexed to heart and triangular shaped gyrase displaying 'full' binding. No systematic difference was detected between views. (c) DNA complexed to heart and triangular views of gyrase displaying 'half' binding. (d) According to disposition of DNA tails on lozenge shaped gyrase, DNA lengths are distributed into two subpopulations that display full binding (empty drawing) and half binding (black drawing) respectively.

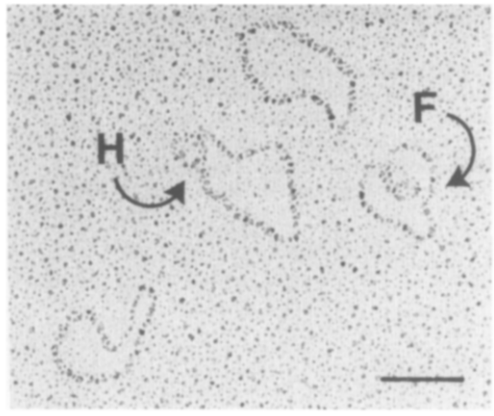

Figure 10. Complex of Gyrase with Closed DNA Circle

Field shows covalently closed 541 bp DNA restriction fragments complexed to gyrase in 'full' (F) or 'half' (H) binding mode. Free DNA included as control. Bar: 500 Å.

posed on comparable images of free gyrase (Figure 2G). A volume of 0.3–0.4 × 10^6 Å^3 would accommodate 140 bp of hydrated DNA (1 g H_2O/g DNA; Bloomfield et al., 1974). The protein itself is hydrated, and the water of hydration is probably replaced by glycerol during the preparation for shadowing. The volume of 0.5 g H_2O/g protein (a typical value) is 0.35 × 10^6 Å^3. Finally, if the views increase in area as a result of flattening of the molecule during drying, there will be an increase in the apparent volume of a reconstructed image. The reasonable agreement between observed and expected volume, after allowing for internal spaces and hydration, suggests that lateral distortions due to flattening are not severe.

Comparison of the images of A subunit dimers and gyrase holoenzyme indicates that the A_2 structure forms the upper portion of the molecule, including the 'ears.' This is illustrated in Figure 2. The remainder of the structure is formed by the two B subunits. Cross-linking of B to B in gyrase was not observed in the experiments of Klevan and Wang (1980), suggesting an absence of specific dimer contacts. The images in Figure 6 also suggest a globular monomer with a strong tendency to aggregate. We have therefore made the schematic assignment shown in Figure 14a. If the B subunits do not make strong contacts with each other, there can be a cleft between them to accommodate DNA.

The DNA-Gyrase Complex

About 140 bp of DNA complexed to gyrase are partially or completely protected from digestion by nucleases corresponding to a contour length of about 480 Å. Since the mean diameter of the gyrase molecule is about 150 Å (this work), DNA must be wrapped in some fashion on or within the protein oligomer. For this reason, we can select those images of the complex with an apparent length decrement of ~120–130 bp as representing the mode of DNA binding

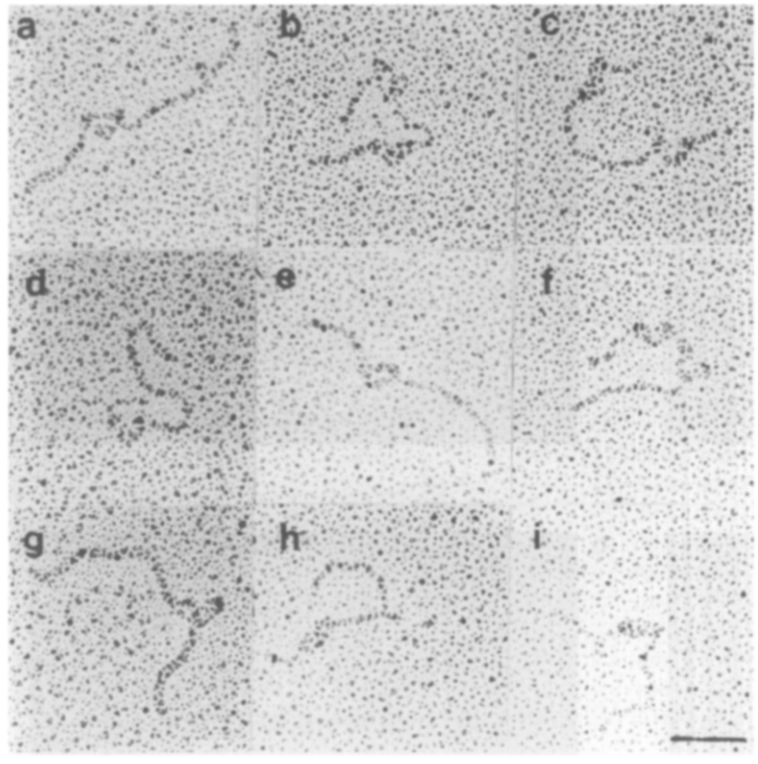

Figure 11. Selected Images of A Subunit Complexed with a 541 bp DNA Restriction Fragment

Images show representative Pt shadowed complexes with no significant length decrement of DNA. (a–g) 'V' shaped view of A_2 dimers; (h and i) Rod-like view of A_2 dimer. Bar: 500 Å.

that corresponds to the nuclease protection studies. We note that the gyrase molecules in such images are not noticeably different from free gyrase, suggesting that the DNA coils largely into grooves or cavities and that the gyrase does not undergo a dramatic conformational change when it binds to DNA. A simple model for the path of DNA in the complex is shown in Figure 13 and in Figure 14. This model accounts for the appearance of gyrase-A_2 complexes as well as for the way in which DNA emerges from the complete A_2B_2 structure. The representation in Figure 13 shows 115 bp of DNA. It is clear that the dimensions of the molecule are appropriate for the protection of up to 140 bp. The model accounts for all the principal features of the DNAase I protection pattern. The central, fully protected zone of about 40–50 bp corresponds to the stretch of DNA shown bound to the two A subunits across the molecular dyad. Since each A subunit is covalently bound to a 5′ end after a double-strand break, the cleavage site must be across this 2-fold axis. The peripheral 40–50 bp on either side of the protected zone are accessible to DNAase I from one side only, and in the model they run near the outside of a groove or cavity between B subunits. Our data do not rule out a model in which the peripheral segments run along a groove in the outer surface of the B subunits, rather than in a slot between them. In the model, B subunits interact only with flanking regions of the 140–150 bp segment. This feature can be tested by DNA–protein cross-linking experiments. The DNA has been drawn as a right-handed supercoil in the complex. If a covalently closed circular DNA is relaxed in the presence of bound gyrase, its linking number is higher by 0.3 to 1.0 per bound gyrase, compared with the same DNA relaxed in the absence of gyrase (Liu and Wang,

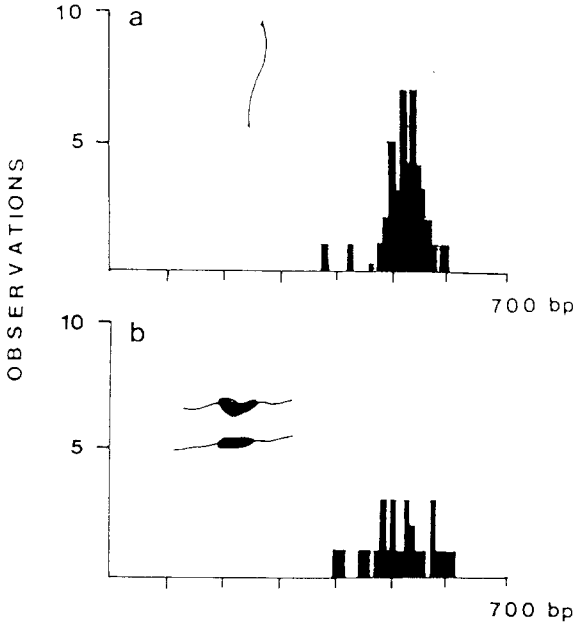

Figure 12. Distribution of DNA Length When Complexed to A Subunits of Gyrase

(a) Length distribution of naked DNA control, the 541 bp restriction fragment used in experiment; (b) length distribution of DNA complexed to A dimer. There is no significant decrement in length. Fragments were traced following a straight line between the exit points along the rod (top view) or along the arms of the 'V' shaped dimer (side view).

1978a; Cozzarelli, 1980; Gellert, 1981b; Klevan and Wang, unpublished results). The simplest explanation of such a result is right-handed coiling without major distortion of the double helix itself. The illustration in Figure 13

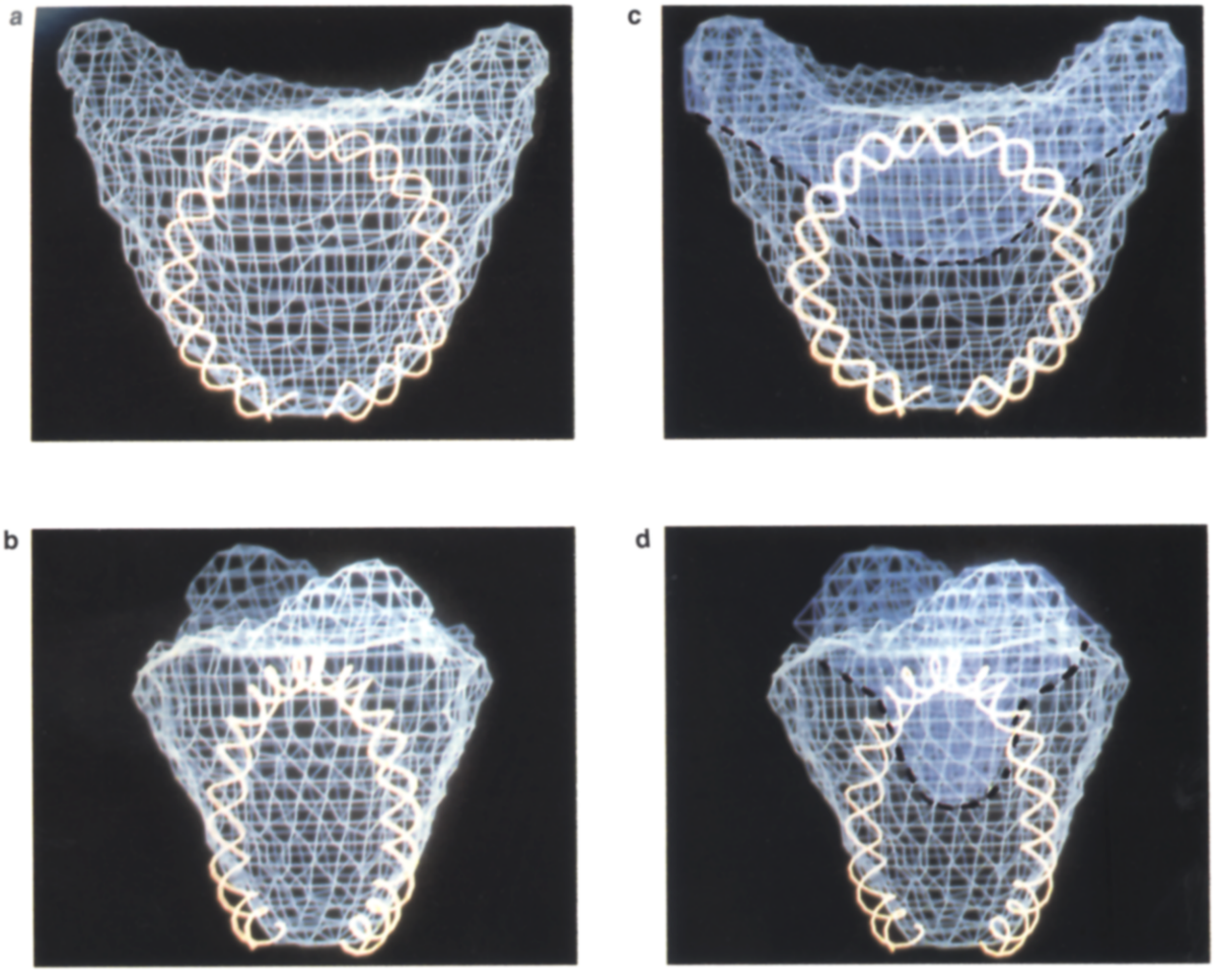

Figure 13. Model Described in Figure 2, with a DNA Backbone Superposed

The DNA coil represents 115 bp, forming a gentle coil. (a and b) Model of holoenzyme and DNA backbone. (c and d) As in (a and b), but with reconstruction of the A dimer added, the views are near 90° (a and c) and 180° (b and d).

shows a uniformly curved DNA, but this aspect is of course purely schematic. The radius of curvature in the representation is 65 Å, and the picture therefore illustrates that a 120–140 bp coil of DNA can reasonably be accommodated within a gyrase molecule, with appropriate peripheral edges accessible.

Relation of the Structure to Mechanism of Action of DNA Gyrase

The action of gyrase corresponds to the introduction of a double-strand break as shown in Figure 14d, passage of another DNA duplex (e.g., another segment of the closed circle to which gyrase is bound) through the gap, and reformation of the broken phosphodiester bonds. Simple passage of duplex DNA through the break generated at the 2-fold axis of the complex requires separation of the ends of that break by at least 30 Å. Moreover, to pass the second duplex completely along the dyad, the A subunits, to which the DNA ends are attached, are likely to lose contact with each other. Concomitant formation of B–B contacts, perhaps near the lower tip of the molecule, is the simplest way to imagine maintaining an intact structure (Figures 14b and 14d). The conformational change in the oligomer is therefore expected to be substantial, although not necessarily of a magnitude detectable in the platinum-shadowed images. We see no evidence for dramatically different forms in the gyrase bound to DNA, but we do not know whether any of the images show gyrase in the state with separated A subunits.

Known activities of gyrase include introduction of negative supercoils (ATP-dependent), relaxation of negative supercoils (ATP-independent), and catenation/decatenation and unknotting of duplex DNA rings (Cozzarelli, 1980; Gellert, 1981b). The catenation/decatenation reaction involves two circular DNA molecules; the other reactions involve one DNA molecule. Formally, the introduction of negative supercoils (and relaxation of positive supercoils) involves passage of some part of the closed circle of DNA through the break introduced by A subunits, in the direction shown in Figures 14h, 14j, and 14k. If the segment passing through the break is at some distance from the segment bound to the A subunits, two loops will form (Figures 14h and 14j). Despite several attempts, we have been unable to detect such loops with circular or linear

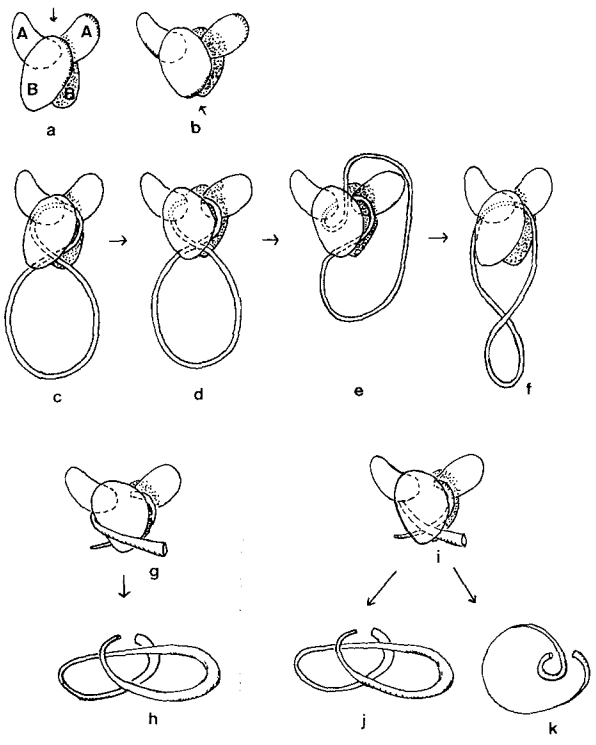

Figure 14. Possible Conformational States of DNA Gyrase and of the Gyrase–DNA Complex

(a) Schematic representation of arrangement of A and B subunits in DNA gyrase, viewed near 135°. (b) Same view as in (a), but with an open A–A contact and a closed B–B contact. (c) and (d) are the same as (a) and (b), but with DNA added. The loop of DNA is shown contained between lobes of the two B subunits. Alternatively, in (g), the arms of the DNA loop pass across the outer surface of the B subunits. Note that opening the A–A contact in (d) involves double-strand scission. (g–h) show one way in which strand passage can occur. A segment of the closed circular DNA passes through the open A–A contact and through the double-strand break. The gyrase molecule is omitted in (h) for clarity. This picture is consistent with either mode of B subunit/DNA interaction, as illustrated in (i) and (j). Completion of a reaction following this course would require closing the A–A contact and opening the B–B contact to allow exit of the inserted segment. (d–f) show an alternative picture, consistent only with the B subunit/DNA binding mode shown in (d) and (i). One of the two arms of the DNA loop, constrained between B subunits and trapped by closure of the B–B contact, diffuses through the double-strand break (e). Completion of the reaction cycle requires rearrangement of the DNA after strand passages, closure of the A–A contact to open the B–B contact (f), and reformation of a bound DNA loop as in (d).

DNA of sizes ranging from several hundred to several thousand bp. Moore et al. (1983) have detected multiple loops in glutaraldehyde-fixed gyrase–DNA complexes; frequently, three or more loops were seen emanating from gyrase bound to a closed circular plasmid. The models in Figures 14g and 14h, or in Figures 14i and 14j, predict at most two loops, if the arc to the segment crossing the DNA gate is sufficiently long to show as a loop in an electron micrograph. In the limiting case, the crossing segment could be directly adjacent to, or even a part of, the 140 bp nuclease-resistant sequence. In this limiting case (Figures 14d–14f and Figures 14i and 14k), there would be only one loop for the entire circular DNA. The one-loop scheme drawn in Figures 14c–14f eliminates an absolute requirement for recruiting a distant strand-passage segment and represents a way of achieving topological specificity through purely local interactions. It can occur only if the flanking sequences of the bound DNA coil lie between the B subunits, as in Figure 14i, rather than across their surfaces, as in Figure 14g. The one-loop structure avoids the possibility of knotting that can result from the scheme shown in Figures 14h and 14j, if the DNA folds back between the enzyme-bound sequence and the strand-passage segment (see Figure 1d of Wang, 1982). Nonetheless, the catenation/decatenation reaction shows that gyrase can under some circumstances pass even an unlinked segment through a double-strand break.

Some of the images of 'incomplete binding modes' could represent the structure expected from Figure 14e, for example. We attempted to trap the strand passage structure by incubating gyrase and DNA in the presence of the β-imido analog of ATP, AMPPNP, since such nonhydrolyzable analogs have been shown to permit introduction of two negative superhelical turns (i.e., one partial cycle; Cozzarelli, 1980; Gellert, 1981b). We were unable to detect a difference, however, in the structures seen by microscopy in the presence or absence of the ATP analog.

The structure of gyrase and the mode of DNA binding that we have deduced are consistent with a number of models for gyrase action. For example, the structures in Figures 14g and 14h correspond respectively to the 'outside,' and 'inside' states of the model for gyrase action proposed by Wang et al. (1980). This and other models have been described in terms of two 'gates,' a 'DNA gate' and a 'protein gate.' In Figure 14, we can describe the A–A dimer contact and its associated DNA as a DNA gate, and the putative B–B contact as a protein gate. Then in the mechanism of Figures 14g and 14h, the protein gate would open after the strand passage to complete a cycle. In Figures 14c–14f, however, DNA in effect first crosses the protein gate, which closes behind it, and protein gate passage thus precedes DNA gate passage in this sequence. Distinguishing between such alternatives will require trapping and visualizing the strand-passage intermediate.

Experimental Procedures

Preparation of Gyrase and Its Subunits

DNA gyrase holoenzyme and the gyrase A subunit of Micrococcus luteus were prepared as previously described (Klevan and Wang, 1980). They were stored as stock solutions of 0.3 mg/ml and 1.1 mg/ml, respectively at −20°C in 0.01 M Tris-HCl (pH 8), 1 mM Na_3 EDTA. For some experiments, Gyrase A and B subunits of Escherichia coli and the reconstituted holoenzyme were kindly supplied by David Horowitz. They were obtained from overproducing strains containing separated *gyr* A and *gyr* B genes cloned on multicopy plasmids, using purification procedures to be published elsewhere.

Preparation of DNA Fragments

A 541 bp Hind III restriction fragment obtained from plasmid pDH8 (Horowitz and Wang, 1984) was used in most of the work described here. The fragment was isolated by polyacrylamide electrophoresis, followed by electroelution of the gel slice containing the DNA and alcohol precipitation. In some of the experiments, the nicked circular form

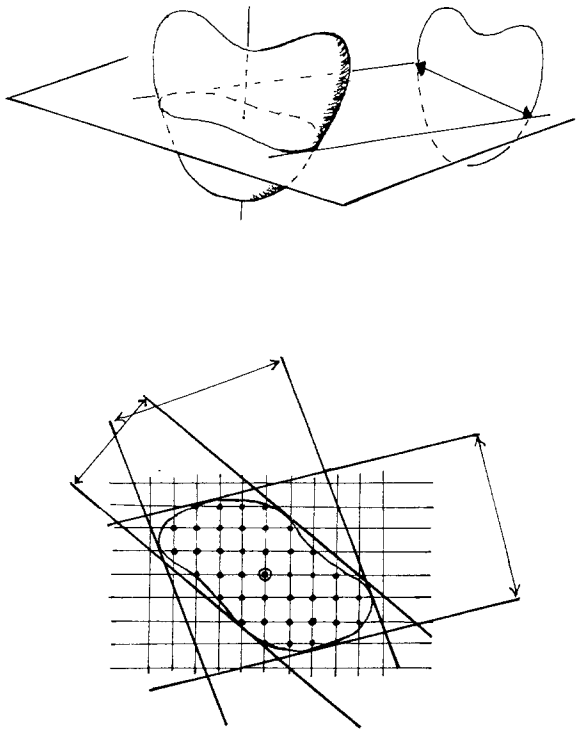

Figure 15. Real-Space Reconstruction of the Envelope of an Object from a Set of Projected Outlines Viewed Normal to a Single Axis

The diagram shows a cross section perpendicular to the axis. The object can be approximated by including only those grid squares that project to all of the observed views (solid dots). In practice, we can allow for some error by including within the computed envelope any grid point that projects within the outline of (n − 1) out of n views, provided that n is sufficiently large.

of the fragment was used. The linear fragment was first converted to the covalently closed circular form by treatment with phage T4 DNA ligase; the gel purified circular monomer was then treated with pancreatic DNAase I to introduce 1–2 single-stranded scissions per molecule, and the nicked and closed circular forms were separated by polyacrylamide gel electrophoresis in the presence of ethidium (Horowitz and Wang, 1984). DNA fragments were stored at about 50 μg/ml in 0.01 M Tris-HCl (pH 8) and 1 mM EDTA at 4°C.

Formation of DNA-Protein Complexes

Typically, 3 μl of gyrase was mixed with 2–5 μl DNA and incubated at 35°C–38°C for 30 min. The reaction mixture was then gently mixed with 35 μl of a solution containing 45% glycerol, 50 mM ammonium acetate (pH 7.0; kept at room temperature) and was immediately processed for electron microscopy.

Electron Microscopy

Single molecules of free gyrase, its subunits, and their complexes to DNA were visualized by electron microscopy after rotary shadowing with platinum. The samples (in 45% glycerol and 50 mM ammonium acetate, pH 7.0) were sprayed onto freshly cleaved mica, dried at reduced pressure, and rotary shadowed lightly with platinum at a glancing angle of 6°–8° (Fowler and Erickson, 1979). Negatively stained samples of A subunit were prepared by adsorption onto freshly glow-discharged carbon-film coated grids, stained with a few drops of 1.5% uranyl acetate, and blot dried. Grids were examined at 80 kV in a JEOL 100 CXII electron microscope. The micrographs have been printed so that the shadowed objects appear to lie facing the viewer on the 'upper' surface of mica. For analysis, images were enlarged from the negatives with a camera lucida. DNA lengths were measured with a digitizing tablet (Evans and Sutherland Multi-Picture System). Negatively stained T4 bacteriophage tails with 41 Å of repeat distance were used as a magnification standard.

Model Stimulation

To facilitate the three-dimensional representation of gyrase, a graphic simulation was obtained from a simple real-space reconstruction of the molecular envelope. The analysis is based on the assumption that the different types of images observed in fields of rotary shadowed molecules are produced by a single rigid structure that adsorbs to the mica surface in different orientations. Rotary shadowing produces an image with an outline that corresponds to a projection of the molecular envelope. Under the condition that the shadow outline indeed corresponds to such a projection, an approximation to the three-dimensional envelope can be computed from a series of views about an axis (Figure 15). Indentations or flutings parallel to that axis will be filled in, and the volume may be somewhat augmented by 'corners' arising from a limited number of projections. The problem is similar to one in the theory of visual perception treated by Marr (1977). We used the characteristic and unusual shape of gyrase (see Figure 1) to select images of molecules viewed normal to their molecular dyad. Two criteria were applied in the selection: that the image should appear symmetric, and that it should be of full length from 'bottom' to 'ears'. The latter criterion was particularly useful, since the longest dimension of gyrase is parallel to the dyad, and images with a height equal to this maximum must therefore correspond to normal views. The azimuth of view about the dyad was calculated from the apparent separation of the ears. Views with maximal ear separation were designated as 90° views, those with ears superposed, as 0° (or 180°) views. The ambiguity for intermediate views (e.g., 45° or 135°) was resolved by noticing that there were two types of images in a given ear separation, 'tapered' and 'bulged' (see Figure 1). We assigned 'bulged' images to the range 0°–90° and 'tapered' images to the range 90°–180°. The choice corresponds to an arbitrary decision about the hand of the molecular envelope. Coordinates of the shadowed outline were read from traced, enlarged images on a relatively fine grid. The outlines of 10–13 views were read by a program that computed the three-dimensional reconstruction and put it out in a format similar to a crystallographic electron density map. This map was displayed on an Evans and Sutherland PS-300 using the program FRODO (Jones, 1978).

Acknowledgments

We thank D. Horowitz for kindly supplying gyrase A and B subunits of Escherichia coli and the reconstituted holoenzyme. We also thank K. Kirkegaard, D. Horowitz, and R. A. Crowther for helpful discussions and suggestions. The work was supported by NSF Grant PCM 82-02821 (to S. C. H.) and by NIH Grant GM-24544 (to J. C. W.).

The costs of publication of this article were defrayed in part by the payment of page charges. This article must therefore be hereby marked *"advertisement"* in accordance with 18 U.S.C. Section 1734 solely to indicate this fact.

Received January 25, 1985; revised April 30, 1985

References

Bloomfield, V. A., Crothers, D. M., and Tinoco, I., Jr. (1974). Physical Chemistry of Nucleic Acids (New York: Harper and Row), pp. 373–476.

Brown, P. O., and Cozzarelli, N. R. (1979). A sign inversion mechanism for enzymatic supercoiling of DNA. Science *206*, 1081–1083.

Cozzarelli, N. R. (1980). DNA gyrase and the supercoiling of DNA. Science *207*, 953–961.

Fisher, L. M., Mizuuchi, K., O'Dea, M. H., Ohmori, H., and Gellert, M. (1981). Site-specific interaction of DNA gyrase with DNA. Proc. Natl. Acad. Sci. USA *78*, 4165–4169.

Fowler, W. E., and Erickson, H. P. (1979). Trinodular structure of fibrinogen-confirmation by both shadowing and negative-stain electron microscopy. J. Mol. Biol. *134*, 241–249.

Gellert, M. (1981a). DNA Topoisomerases. Ann. Rev. Biochem. *50*, 879–910.

Gellert, M. (1981b). DNA gyrase and other type II DNA topoisomerases. The Enzymes 14 (New York: Academic Press), pp. 345–366.

Gellert, M., Mizuuchi, K., O'Dea, M. H., and Nash, H. A. (1976). DNA gyrase: an enzyme that introduces superhelical turns into DNA. Proc. Natl. Acad. Sci. USA *73*, 3872–3876.

Gellert, M., Mizuuchi, K., O'Dea, M. H., Itoh, T., and Tomizawa, J. (1977). Nalidixic acid resistance: a second genetic character involved in DNA gyrase activity. Proc. Natl. Acad. Sci. USA *74*, 4772–4776.

Horowitz, D., and Wang, J. C. (1984). Torsional rigidity of DNA and length dependence of the free energy of DNA supercoiling. J. Mol. Biol. *173*, 75–91.

Jones, T. A. (1978). A graphics model building and refinement system for macromolecules. J. Appl. Crystallography *11*, 268–272.

Kirkegaard, K., and Wang, J. C. (1981). Mapping the topography of DNA wrapped around gyrase by nucleolytic and chemical probing of complexes of unique DNA sequences. Cell *23*, 721–729.

Klevan, L., and Wang, J. C. (1980). A DNA–DNA gyrase complex containing 140 base pairs of DNA and an $\alpha_2\beta_2$ protein core. Biochemistry *19*, 5229–5234.

Kreuzer, K. N., and Cozzarelli, N. R. (1980). Formation and resolution of DNA catenanes by DNA gyrase. Cell *20*, 245–254.

Liu, L. F., and Wang, J. C. (1978a). DNA–DNA gyrase complex: the wrapping of the DNA duplex outside the enzyme. Cell *15*, 979–984.

Liu, L. F., and Wang, J. C. (1978b). Micrococcus luteus DNA gyrase: active components and a model for its supercoiling of DNA. Proc. Natl. Acad. Sci. USA *75*, 2098–2102.

Liu, L. F., Liu, C.-C., and Alberts, B. M. (1980). Type II DNA topoisomerases: enzymes that can unknot a topologically knotted DNA molecule via a reversible double-strand break. Cell *19*, 697–708.

Lother, H., Lurz, R., and Orr, E. (1984). DNA binding and antigenic specifications of DNA gyrase. Nucl. Acids Res. *12*, 901–914.

Marr, D. (1977). Analysis of occluding contour. Proc. Roy. Soc. B *197*, 441–475.

Mizuuchi, K., Fisher, L. M., O'Dea, M. H., and Gellert, M. (1980). DNA gyrase action involves the introduction of transient double-strand breaks into DNA. Proc. Natl. Acad. Sci. USA *77*, 1847–1851.

Moore, C. L., Klevan, L., Wang, J. C., and Griffith, J. D. (1983). Gyrase–DNA complexes visualized as looped structures by electron microscopy. J. Biol. Chem. *258*, 4612–4617.

Morrison, A., and Cozzarelli, N. R. (1979). Site-specific cleavage of DNA by E. coli DNA gyrase. Cell *17*, 175–184.

Morrison, A., and Cozzarelli, N. R. (1981). Contacts between DNA gyrase and its binding site onto DNA: features of symmetry and asymmetry revealed by protection from nucleases. Proc. Natl. Acad. Sci. USA *78*, 1416–1420.

Morrison, A., Higgins, N. P., and Cozzarelli, N. R. (1980). Interactions between DNA gyrase and its cleavage site on DNA. J. Biol. Chem. *255*, 2211–2219.

Nash, H. A., Mizuuchi, K., Weisberg, R. A., Kikuchi, Y., and Gellert, M. (1977). Integrative recombination of bacteriophage λ—the biochemical approach to DNA. In DNA Insertion Elements, Plasmids and Episomes, A. I. Bukhari, ed. (Cold Spring Harbor, New York: Cold Spring Harbor Laboratory), pp. 363–374.

Sugino, A., Peebles, C. L., Kreuzer, K. N., and Cozzarelli, N. R. (1977). Mechanism of action of nalidixic acid: purification of *Escherichia coli nalA* gene product and its relationship to DNA gyrase and a novel nicking-closing enzyme. Proc. Natl. Acad. Sci. USA *74*, 4767–4771.

Sugino, A., Higgins, N. P., and Cozzarelli, N. R. (1980). DNA gyrase subunit stoichiometry and the covalent attachment of subunit A to DNA during DNA cleavage. Nucl. Acids Res. *8*, 3865–3874.

Tse, Y.-C., Kirkegaard, K., and Wang, J. C. (1980). Covalent bonds between protein and DNA. J. Biol. Chem. *255*, 5560–5565.

Wang, J. C. (1982). The application of recombinant DNA methods to structural studies of DNA. In Nucleases, R. Roberts and S. Linn, eds. (Cold Spring Harbor, New York: Cold Spring Harbor Laboratory), pp. 41–57.

Wang, J. C. (1985). DNA Topoisomerases. Ann. Rev. Biochem. *54*, 665–697.

Wang, J. C., Gumport, R. I., Javaherian, K. J., Kirkegaard, K., Klevan, L., Kotewicz, M. L., and Tse, R.-C. (1980). DNA topoisomerases. In Mechanistic Studies of DNA Replication and Genetic Recombination (ICN-UCLA Symposia on Molecular and Cellular Biology *19*). B. M. Alberts and C. F. Fox, eds. (New York: Academic Press), pp. 769–784.